Report on project

ÅForsk Foundation, ref. nr 23-216

The role of potassium (K) on formation of soot from biomass combustion, and impact on climate and health

Summary

The influence of potassium on soot formation has been studied in detail in laboratory flames using a variety of techniques which probes various properties. All techniques were based on sampling soot in the flames either in gas phase or on a probe. The flames were operated with or without potassium seeded into the flames. The interest in potassium originates from high potassium concentrations in biomass and the lack of knowledge on soot formation during biomass burning. The main results are the following; (1) Potassium leads to soot that is less absorbing, i.e. is more brownish, and tend to have a more organic character, (2) Potassium also leads to clearly smaller soot particles, (3) Raman spectroscopy shows similarity in spectra between the reference case and the potassium-seeded case indicating that the internal bonding structure is relatively similar for both cases, and (4) X-ray photoelectron spectroscopy (XPS) data from measurements at MAX IV showed an increased sp^2-hybridization in relation to sp^3-hybridization on the soot surface with potassium addition. **To summarize the results, the lower absorption and the smaller particle sizes as a result of potassium is beneficial for the climate effects of soot originating from biomass burning. The lower absorption means that the global warming effect is less for this soot produced influenced by potassium, and the smaller particles can be beneficial due to a faster and more effective burnout of soot during wildfires.**

Project background

Soot particles emitted from forest fires, domestic heating, cook stoves, engines, and industrial processes lead to serious health effects and contribute to global warming. These emitted soot particles show a variety of properties, for example regarding size, bonding structure, and chemical composition. This project aims generally to shed light on the influence of potassium on soot formation in various combustion processes. The interest in potassium addition originates from previous investigations that suggest a correlation between potassium addition and soot formation. Furthermore, biofuels contain significant amounts of potassium.

The project aims to investigate and explain the changes in characteristic soot properties resulting from potassium addition to the fuel. This knowledge will increase the understanding of the impact on health, environment, and climate, from soot, with various amounts of added potassium to the fuel. In the longer perspective it would be interesting to know if intentional potassium addition in combustion can lead to lower soot concentrations and less contribution of soot to global warming.

Non-intrusive advanced optical techniques were combined with sampling of soot and subsequent ex-situ analysis in laboratory flames, with various amounts of potassium seeded into the flames. Different characteristic properties of the soot from fuel with and without seeding of soot has been compared. The results will generally contribute to the understanding about how the properties of different types of soot contribute to respiratory diseases and to global warming.

The present project adds important information to previous work on the impact of potassium on soot formation [1-4]. The results from the present work are presented in the PhD thesis of Saga Bergqvist [5] defended on January 17 2025, and in a manuscript submitted to Aerosol Science and Technology in December 2024 [6].

Methods

The soot particles were sampled from a modified Perkin-Elmer burner operated with an equivalence ratio of $\Phi = 2.6$ and a cold gas velocity of 7.1 cm/s, see Fig. 1. The flame was stabilized by a stainless steel plate (Ø = 20 mm) placed 21 mm above the burner surface. This burner allows for seeding of various solutions into the flame through the air/fuel mixture. In this study, a salt solution of KCl dissolved in deionized water of 1 M concentration was used for seeding. For comparison, the flame was seeded with pure deionized water as a reference case.

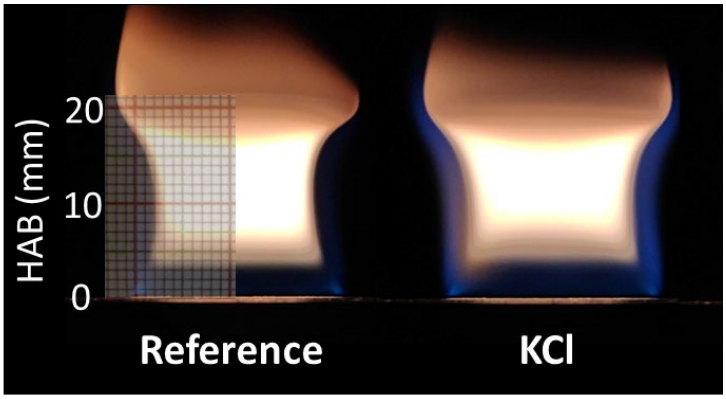

Figure 1: Images of flames from the reference case seeded with deionized water as well as the flame with 1 M addition of KCl.

The soot particles were extracted from the flame at different heights using a water cooled, stainless steel sampling probe, see Fig. 2. The probe consists of a stainless-steel pipe with an outer diameter of 6 mm placed horizontally across the flame with water cooling around the pipe outside of the flame region. The particles enter the probe through a small orifice (diameter, Ø = 1 mm) pointing downwards in the flame and are immediately quenched by a high nitrogen (N_2) flow. The particles were collected downstream on a quartz fiber filter (Whatman QM-A, Ø = 25 mm) for ex-situ studies using various techniques presented in the results section.

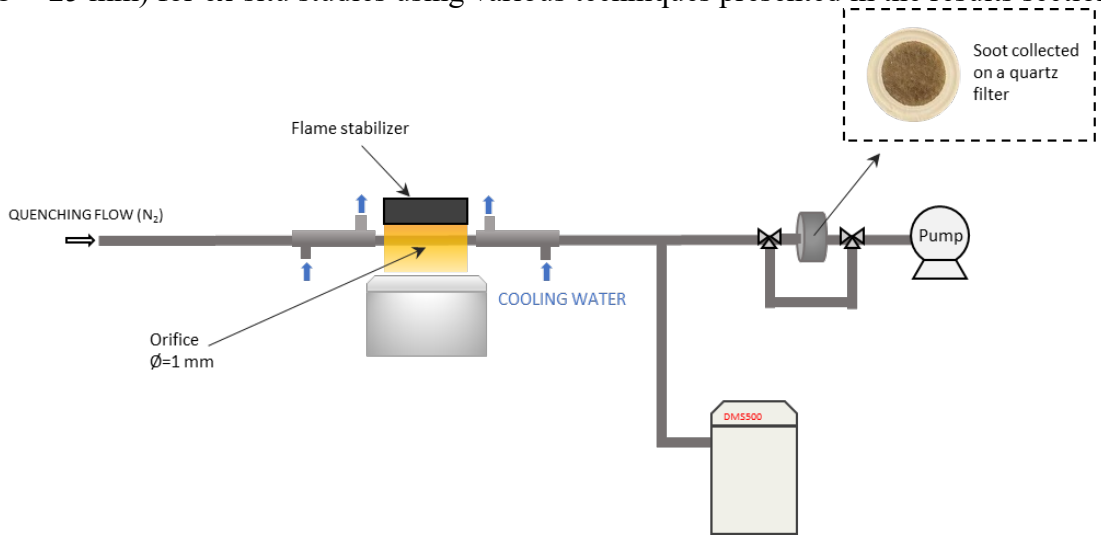

Figure 2: Soot sampling system and soot collection equipment.

Project results

Thermo-optical analysis

The organic, elemental, and total carbon concentrations (OC, EC, TC), as well as pyrolytic carbon (PC) formed during heat treatment, were determined from the collected quartz filter soot deposits using a Multi-Wavelength Thermal-Optical Carbon Analyzer (MW-TOA; DRI 2015 Series 2, Aerosol Magee Scientific, Slovenia). The instrument continuously measures the reflectance and transmission light intensity of the filter sample at seven wavelengths: 405, 445, 532, 635, 780, 808, and 980 nm, allowing for optical analysis during thermal evolution. Evolved carbon is oxidized to CO_2 in a MnO_2 catalyst oven, after which it is quantified by a nondispersive infrared (NDIR) sensor.

The filter samples were analyzed using the EUSAAR2 TOA protocol. The protocol includes four thermal steps (OC1-OC4) in inert Helium atmosphere (200 °C for 120 s; 300 °C for 150 s; 450 °C for 180 s; and 650 °C for 180 s) followed by a cooldown period to ~500 °C, and finally four thermal evolution steps (EC1-EC4) in a 2 % Oxygen and 98 % Helium atmosphere to help facilitate removal of the remaining carbon from the filter by soot oxidation (500 °C for 120 s; 550 °C for 120 s; 700 °C for 70 s; and 850 °C for 80 s), after which all the carbon has been evolved from the quartz filter. Pyrolytic carbon (PC) is formed by carbonization of organic carbon in the inert He-phase (OC1-OC4).

In Fig. 3, the thermograms for the soot sampled at 14 mm HAB in the modified Perkin-Elmer burner are shown, when seeding the flame with deionized water (Ref, Fig. 3 (a)) and 1 M KCl (Fig. 3 (b)), also presented in [6]. The attenuation at 635 nm (in black) is shown as a function of the measurement time, together with the measurement temperature (dashed, red line) and the NDIR signal related to the evaporated carbon (green). From the attenuation, the absorption Ångström exponent (AAE) using all wavelengths (AAE_{tot}) as well as using high wavelengths (AAE_{high}) are shown in blue and red respectively. It can be seen that the main difference between the two cases is that the optical absorption efficiency is lower for soot with added potassium, despite similar soot loading on both filters.

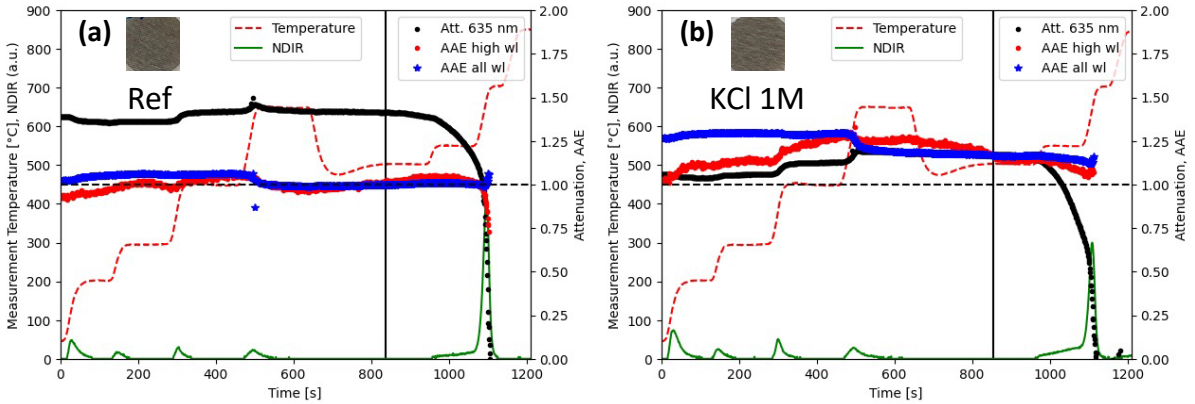

Figure 3: Thermograms of the flame soot with addition of 1 M KCl in (b) and the reference case seeded with pure ionized water (Ref) in (a).

Another observation from Figs 3 (a) and (b) is that the changes in the attenuation during heating of the soot are small, indicating that the soot does not darken significantly during heat treatment. Hence, this shows that the soot is mature and not strongly affected by the heat treatment. It can also be observed that with potassium addition in Fig. 3 (b) that the attenuation increases more with heating in comparison with the reference case, which indicates that potassium addition makes the soot less mature at the sampled position in the flame.

The fractions of OC, PC and EC were derived from the TOA analysis for the samples from the modified Perkin-Elmer burner using deionized water as a reference case and comparing to

seeding with 1 M KCl. The results are shown in Fig. 4 [6]. The soot from the reference case had the highest fraction of EC (75%) and the lowest fraction of OC (25%), the PC fraction was negligible. The sample with 1 M KCl addition, showed a higher OC 38% and a PC fraction of 3.6%. This indicates that the soot with salt addition has a slightly higher organic content than the reference case, which agrees well with the observed changes in attenuation shown in Fig. 3.

The mass absorption coefficient (MAC) at 635 nm was derived from the data in Fig. 3 for the soot with 1 M KCl addition and the reference case and are shown in Fig. 4. Two main observations can be made. The first observation is that MAC for soot with potassium addition has a lower absorption efficiency for the untreated sampled soot in comparison with the sampled soot from the reference case. Secondly, the MAC increases steadily for soot sampled in both cases with and without potassium addition.

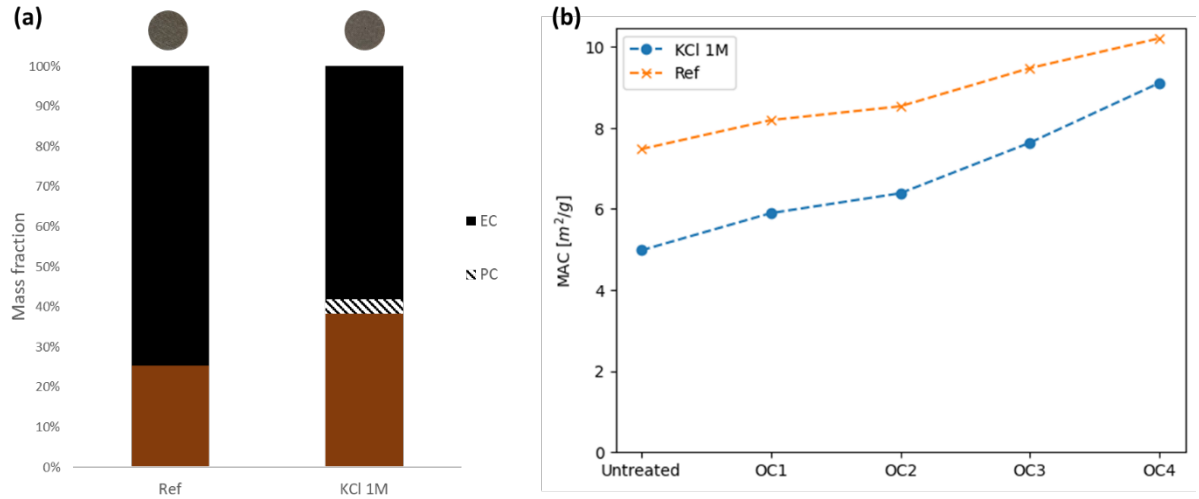

Figure 4: (a) Fractions of organic carbon (OC), pyrolytic carbon (PC) and elemental carbon (EC) derived from the TOA, and (b) MAC values during heating for the two soot samples with 1 M addition of KCl as well as from the reference case [6].

Particle sizing using DMS500

The mobility size distributions were measured using a fast particle sizer (DMS500) during the flame sampling. The size distribution of the particles was observed to shift to smaller sizes upon potassium addition, as seen in Fig. 5. This shift to smaller sizes applied to both the nucleation mode and the accumulation mode. In addition, the concentration of particles in the nucleation mode was drastically decreased with potassium addition. These findings agree with previous studies where potassium addition has been seen to interfere with soot growth and also lead to a decrease in the primary particle size.

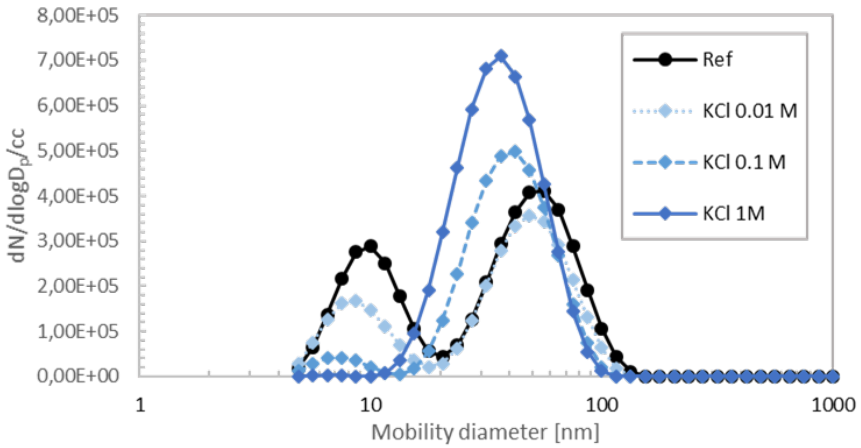

Figure 5: Mobility size distributions of soot from soot forming flames with addition of various amounts of KCl.

Raman spectroscopy

Raman spectra of soot are compared in Fig. 6, both from soot produced with and without potassium addition [5]. Soot was sampled at 14 mm HAB on sapphire glass substrates and was measured ex-situ with an excitation wavelength of 532 nm. The spectra of the reference case (black line) and the case with 1 M KCl addition (red line) appear rather similar with only minor changes. The intensity of the D_3 and D_1 peaks can be observed to increase slightly in relation to the G peak intensity with KCl addition. An increase of the intensity of the D_3 peak indicates an increased content of amorphous carbon, and an increased intensity of the D_1 peak in relation to the G peak intensity is usually attributed to an increased graphitization in soot However, it should be noted that the observed changes are small. Due to the relation between the graphitic unit size and the D_1 to G peak ratio ($I(D_1)/I(G) \sim L_a2$), it can be deducted from the Raman spectra that the graphitic unit size increases slightly with KCl addition due to the observed increase of the D_1 to G peak intensity ratio.

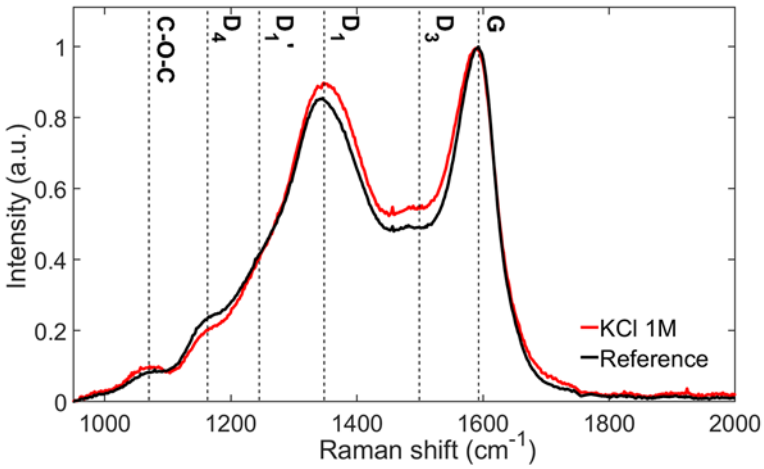

Figure 6: First order Raman spectra of soot with 1 M KCl addition (in red) as well as from the reference case (in black). The spectra are normalized to the G-peak intensity.

The structural changes during heat treatment were studied using Raman spectroscopy of soot with addition of 1 M KCl and soot from the reference case in Fig. 7. The spectra for the

untreated sample are shown in blue, the following curves corresponds to the end of each heating stage, ending with the end of EC3 shown in dark red. During heat treatment there is a slight decrease of the D_1 peak, centered around ~1350 cm^{-1}, in relation to the G-peak in both the soot with addition of 1 M KCl as well as in the reference case. This decrease was observed in the heat treatment in an inert atmosphere ~OC1-OC3 stage, indicating that defects in the graphitic lattice are introduced as a result of the pyrolysis, possible due to breakage of the carbonaceous structure. In addition, a slight decrease can be observed in the D_4 peak around 1200 cm^{-1} in both samples.

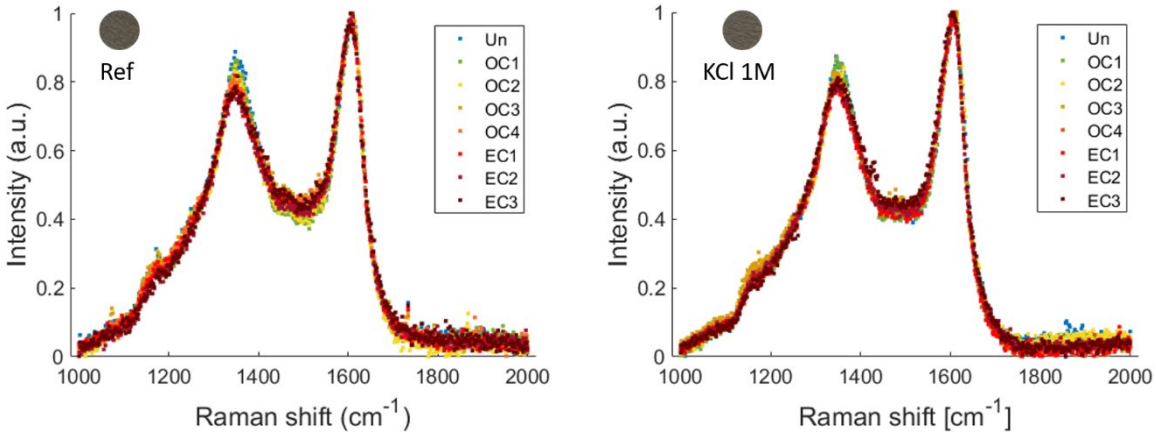

Figure 7: Raman spectra of soot with 1 M KCl addition in (b) and the reference case in (a). The spectra are shown during heating spanning from the untreated case in blue to the end of the EC3 stage in dark red.

X-ray photoelectron spectroscopy (XPS)

Using XPS, the surface structure of the soot can be studied, since the X-rays only penetrate a few nm into the sample surface. The in-flight XPS spectra of the C1s transition measured for soot from the reference case (black circles) and the case with 1 M KCl addition (red stars) are shown in Fig. 8 [5]. Both spectra show a main feature as a prominent peak at ~284.7 eV indicating that the surface is dominated by sp^2 bonded carbon. This is expected for relatively mature soot, which both the soot from the reference case and with 1 M KCl can be assumed to be, based on previous observations. The spectra appear almost identical indicating a similar surface structure of the two soot samples. However, a slight difference can be observed ~285.5 eV at the location for sp^3 bonded carbon, where the intensity of this feature seemed to decrease slightly with KCl addition.

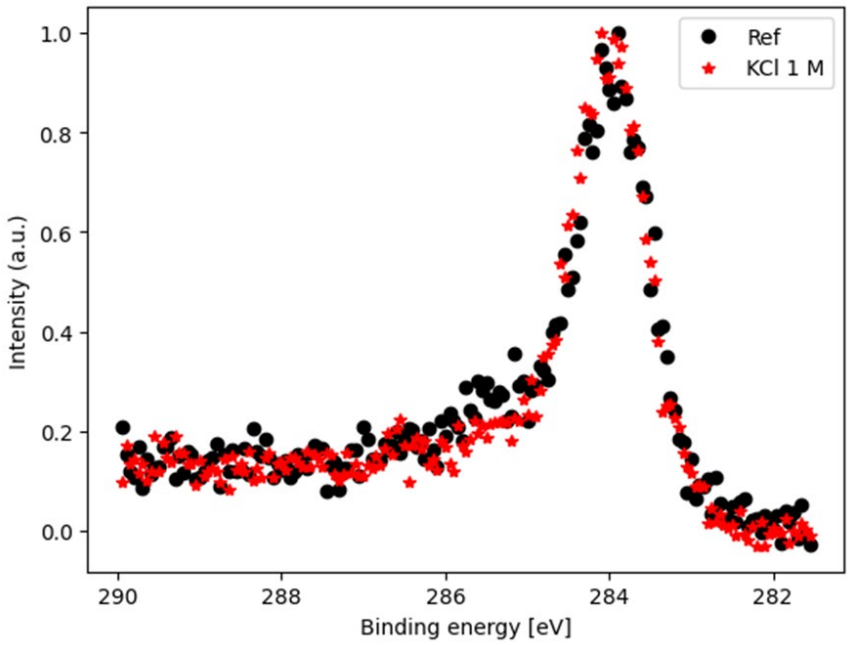

Figure 8: XPS spectra of flame soot from the modified Perkin Elmer burner, sampled at 12 mm HAB with an equivalence ratio of 2.6. The soot produced with 1 M KCl addition is shown in red, and soot from the reference case in black [5].

To better assess the differences between the two spectra, they were deconvoluted using a fit of four Voigt functions and the results are shown in Fig. 9. The deconvoluted spectra shows a clear reduction of the sp^3 peak marked with an orange, dashed line with KCl addition. The sp^2/sp^3 hybridization ratio was computed as the peak area of the deconvoluted and was found to be 2.4 in the reference case and 4.4 in the case with 1 M KCl addition. Hence it seems like the surface of the soot becomes more graphitic with KCl addition.

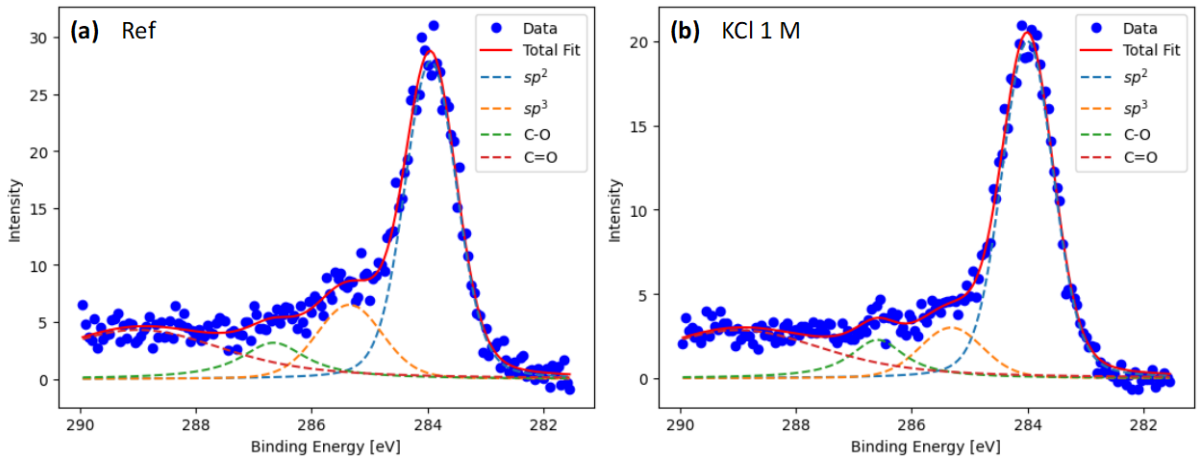

Figure 9: Deconvoluted XPS C1s spectra of soot from the reference case in (a) and from the case with 1 M KCl addition in (b). Four Voigt functions were fitted for the deconvolution.

4. Conclusions

This study investigated absorption properties and structure of soot sampled in flames with the influence of potassium addition. The sampled soot particles were analyzed using a variety of different techniques. The following conclusions can be drawn:

- Thermo optical analysis showed that soot formed with added potassium had a lower absorption efficiency for similar amounts of probed soot. This lower absorption efficiency could also be expressed through the mass absorption coefficient (MAC/ [m^2/g]), which was lower for the soot produced with added potassium.
- During maturation of soot in the soot formation process the organic fraction (OC) of soot decreases and the elemental fraction (EC) increases. It was found that soot formed with added potassium showed a higher organic fraction, i.e. this soot could be considered to be less mature.
- Heat treatment of the soot led to increased MAC-values for soot both with and without potassium addition. However, even at the highest temperature in the inert atmosphere, the absorption was less for the soot with added potassium.
- Mobility particle sizes were measured using a fast particle sizer (DMS500). Addition of potassium in the soot forming flame led to smaller particles sizes for both the nucleation mode and the accumulation mode. Additionally, the nucleation mode was strongly suppressed with increasing potassium concentration.
- Raman spectra probing the bulk carbon structure showed the common D and G-peaks for carbon materials. The changes in the peak ratio between these two peaks were found to be minor when potassium was added to the soot-forming flame. Also heating of the soot resulted in minor changes in the Raman spectra for both cases.
- X-ray photoelectron spectroscopy (XPS) was used to probe the surface structure of soot formed with and without potassium addition. The results showed an increased sp^2-hybridization in relation to sp^3-hybridization on the surface with potassium addition.

5. References

[1] J. Simonsson, N.-E. Olofsson, A. Hosseinnia, P.-E. Bengtsson, Influence of potassium chloride and other metal salts on soot formation studied using imaging LII and ELS, and TEM techniques, *Combustion and Flame* 190 (2018) 188-200.

[2] M. Mannazhi, S. Bergqvist, S. Török, D. Madsen, P. Tóth, K.C. Le, P.-E. Bengtsson, Strongly reduced optical absorption efficiency of soot with addition of potassium chloride in sooting premixed flames, *Proceedings of the Combustion Institute* 39 (1) (2023) 867-876.

[3] M. Mannazhi, S. Bergqvist, P.-E. Bengtsson, Laser-induced fluorescence for studying the influence of potassium and sodium salts on PAH formation in sooting premixed flames, *Applied Physics B* 128 (68) (2022).

[4] M. Mannazhi, S. Bergqvist, P.-E. Bengtsson, Influence of potassium chloride on PAH concentration during soot formation studied using laser-induced fluorescence, *Combustion and Flame* (2021) 111709.

[5] S. Bergqvist, Using light to characterize soot particles and their precursors – from flames to aerosols, PhD thesis, ISBN 978-91-8104-279-5, Media tryck, Lund University

[6] S. Bergqvist, J. Rex, A. Kaarnaa, Cuong Le, A.C. Eriksson, J. Pagels, P.-E. Bengtsson, Flame soot characterization using combined multi-wavelength thermo-optical analysis and Raman spectroscopy, manuscript submitted to *Aerosol Science and Technology* on December 20, 2024.